Stress measurement of a jointed rock mass during drift development

J. C. JOHNSON, M. K. LARSON, T. M. BRADY, & J. K. WHYATT
Spokane Research Laboratory, National Institute for Occupational Safety and Health, Spokane, WA, USA

R. B. LANGSTON, Stillwater Mining Company, Nye, MT, USA

H. KIRSTEN, Steffen Robertson and Kirsten, Johannesburg, South Africa

ABSTRACT: An experiment is described in which hollow inclusion cells (HICells) were used to measure stress in a jointed rock mass during drift development at the Stillwater Mine, Nye, MT, USA. Two HICells were installed in the footwall approximately two drift widths ahead of the face. One HICell was overcored and then immediately tested in a biaxial chamber. The other HICell was left in place and monitored as the drift was excavated in three advances, each one-half the width of the drift. Strains were recorded hourly by a datalogger. Results show that there was little stress change during the first and second drift advances, but that a large stress change occurred after the third advance. The measurements also showed that the in situ principal stress directions lined up with regional geologic structures. Stress changes during face advance were likely caused by deformation along localized joint sets and inelastic deformation near the face.

1. INTRODUCTION

Safety and health are prime concerns of the mining industry. Because ground falls continue to be a major contributor to underground injuries and fatalities across the nation, many mining companies conduct design and stability analyses to reduce or minimize these problems. Investigators at the Spokane Research Laboratory of the National Institute for Occupational Safety and Health (NIOSH) are studying methods to validate computer models of a rock mass in order to advance designs for a safer work environment for miners. One such method is to compare field stress to calculated stress.

An experiment was conducted in the Stillwater Mine, Nye, MT, in which stresses were measured during the advance of the 3200-level footwall drift. Hollow inclusion stress cells (HICells) (Mindata, [1976]) were installed in two holes 6.1 m (20 ft) and 7.2 m (23.5 ft) (about two drift widths) ahead of the face at the extreme eastern end of the drift. In the first hole, a HICell was installed, overcored, and immediately tested in a portable biaxial chamber on site to determine the elastic properties of the rock. In the second hole, which was drilled from a crosscut, a HICell was installed 2.6 m (8.5 ft) from the overcore site to measure stress change during drift advance. The purpose of this paper is to describe the instruments, the installation procedure, and the measured stresses.

2. APPARATUS

The HICell[1] was invented by Worotnicki and Walton (1976). In the 12-gauge version used in this study, three strain gauge rosettes and three single gauges were embedded at various orientations in an thin, hollow epoxy shell.

The HICell was then installed in an EX-size (38.1 mm [1.5 in]) borehole. During installation, a piston forces epoxy from the center cavity into the space between the instrument and the borehole wall. The curing reaction is exothermic, resulting in thermal strains that come to equilibrium before 16 hr has passed.

Although the instrument is known to creep over long periods of time, creep effects were considered to be small because the monitoring period for the second HICell was only 1 week.

3. LOCATION

The Stillwater Mine is a platinum-palladium mine located in south-central Montana about 145 km (90 miles) southwest of Billings, MT. The test site in the mine lies in the middle of a small, narrow valley flanked by large mountains. Mining takes place within a layered igneous body known as the JM Reef in the Stillwater complex. Figure 1 is a plan view of the major geologic features in which the 3200 level is projected to the surface.

Figure 2 is a plan view of the 3200 level. The test area lies near the eastern end of the footwall drift. Actual installation took place when the eastern end of the drift was developed only to the installation area. Figure 3 shows the location of the two HICells.
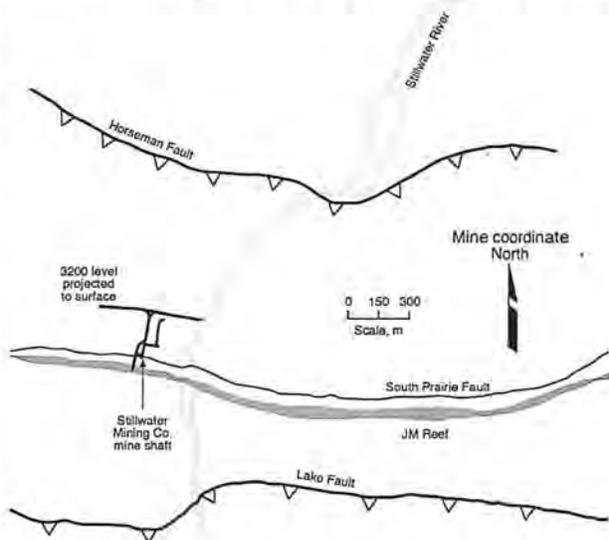

Figure 1.—Plan view showing 3200-level drifts, reef, and nearby major faults. The Horseman and Lake faults are thrust faults. The South Prairie Fault is located near the JM Reef on the hanging wall side, and both are north of the footwall drift of the 3200 level.
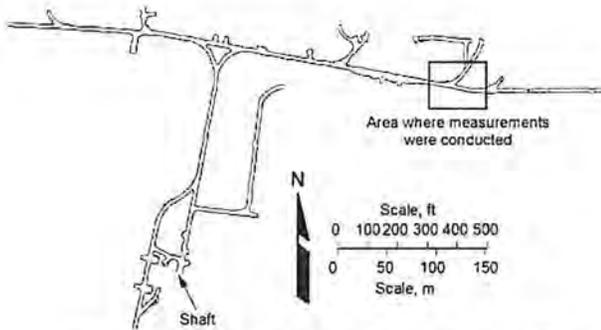

Figure 2.—Plan view of 3200 level showing area where measurements were collected
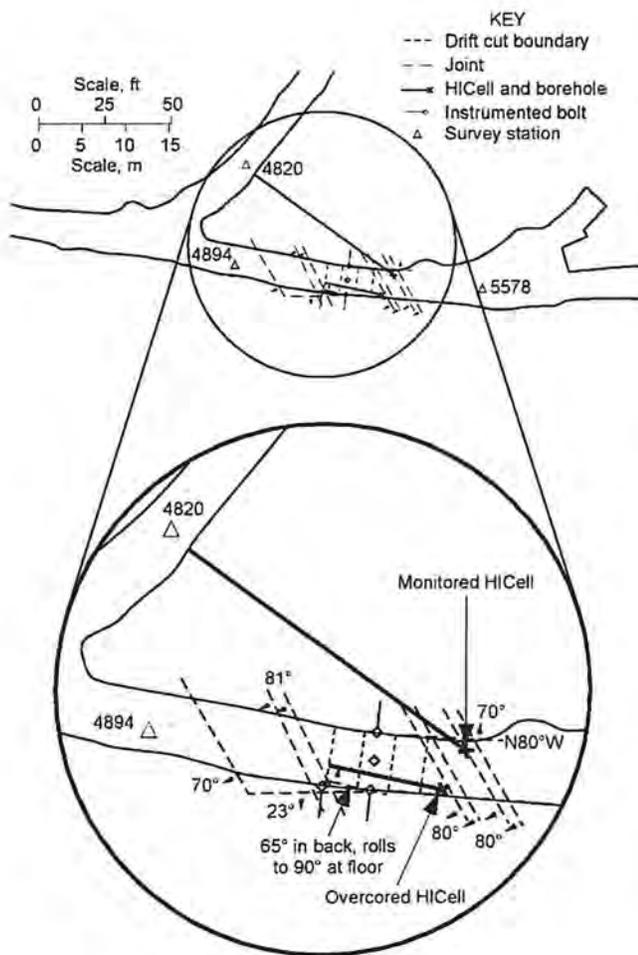

Figure 3.—Plan view of eastern end of 3200-level footwall drift showing location of HICell installations, drift advances, and joints.

4.   SIGN CONVENTION

In this paper, tensile strain and stress are indicated with a positive sign, while compressive strain and stress are denoted with a negative sign. This practice is standard for mechanics, but may be different in many rock engineering circles. In rock mechanics, usually the highest compressive principal stress is labeled the major

principal stress. Using the term major to denote the largest algebraic principal stress may cause confusion. Therefore, in this paper, the authors avoided using the terms major and minor principal stress, but labeled them principal stress PS1, PS2, and PS3 in order of highest to lowest algebraic magnitude.

5.   IN SITU STRESS MEASUREMENT

5.1 *Procedure*

A 152-mm- (6-in-) diameter borehole was drilled to 5.84 m (19 ft, 2 in), and an EX hole was drilled along the same axis for 0.5 m (20 in) more. The HICell was prepared and installed in the EX hole according to standard installation procedures (Mindata 1976). Final placement of the strain gauges was 20.3 cm (8 in) from the EX collar and 6.05 m (19 ft, 10 in) from the drift. The instrument was allowed to cure for 19-1/2 hr before overcoring operations began.

The HICell was monitored with three strain indicators. A 10-channel, switch-and-balance box was connected to the first strain indicator so that readings from all twelve strain gauges could be recorded. The drill water was turned on and allowed to run for 10 min to reach a temperature equilibrium. During overcore drilling, gauge readings were taken at 5-cm (2-in) intervals. Once drilling ceased, the water was allowed to run until readings stabilized.

Upon removal from the borehole, the overcore was placed in a biaxial chamber. The chamber was pressurized in -0.69-MPa (-100-psi) increments up to -6.89 MPa (-1000 psi) for the first loading cycle. HICell strain gauges were monitored at each load. A second loading cycle was begun at -3.45 MPa (-500 psi) and went to -10.3 MPa (-1500) psi. A third and a fourth loading cycle went from 0 to -10.3 MPa (-1500 psi) in -3.45-MPa (-500-psi) increments.

5.2 *Results*

Figure 4 shows strains as a function of distance between the drill bit and the centerlines of the strain gauge rosettes. The first three scans were taken before drilling began, and the last three scans were taken after drilling ceased. For convenience, these readings are shown in Figure 4 at distances of ±27.9, ±25.4, and ±22.9 cm (±11, ±10, and ±9 in) from the centerlines of the rosettes. Overcoring strain changes were calculated by taking the difference between initial and final measurements. Initial measurements were considered those taken after the drilling water had been running for 10 min but before drilling began. "Final" measurements were considered to be those collected last as readings stabilized. Table 1 lists initial and final strains and changes in strain during overcoring. A plot of strain versus applied biaxial pressure is shown in Figure 5. The figure shows linear, isotropic behavior.

Elastic material constants were fit to biaxial test strains using the least squares method. Ideally, the strains used in this fit should be those measured at the stress level that most closely reflected the expected stress state relieved. Because of equipment limitations, the maximum applied stress level was only -10.3 MPa (-1500 psi), which was less than the expected overburden stress. Because a secant modulus was desired, only strains measured at 0 and -10.3 MPa (-1500 psi) were used to calculate biaxial test strain changes. These values are shown in Table 2.
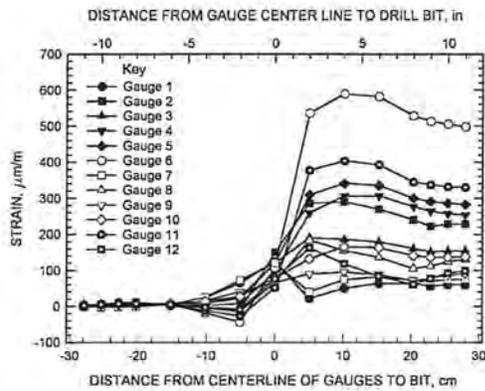
Figure 4.—Overcoring strains versus distance of drill bit to centerline of gauges
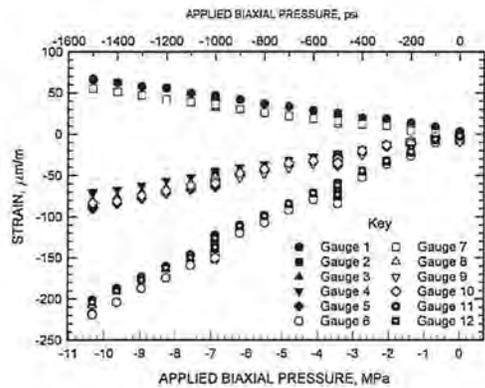

Figure 5 .—Applied biaxial pressure versus measured strain in HICell during biaxial compression test

Elastic constants were determined from the biaxial test with a least squares fit using the computer program STRESsOUT (Larson, 1992) and checked with the computer program STRESS91 (Mindata, 1990). Young's modulus was calculated as 122 GPa (17,700,000 psi), and Poisson's ratio was calculated as 0.31. The correlation coefficient, r^2, was 0.98.

Stress tensors were fit in a drift coordinate system, as shown in Figure 6. The borehole azimuth was 2°, and borehole inclination was 4° above horizontal.

The stress tensor was fit with the program STRESsOUT and checked using the code STRESS91. Table 3 lists stress components calculated in the two coordinate systems. Table 4 lists principal stresses and directions. The correlation coefficient, r^2, was 1.00 using all strain changes in the fit. Standard errors of the stress components ranged from 0.8% to 3.7% of the highest compressive principal stress. The high correlation coefficient and low standard errors indicate a good quality measurement and linear, homogeneous material.

6.   STRESS CHANGE MEASUREMENT

6.1 *Procedure*

The instrument was prepared and installed according to standard installation procedures (Mindata [1976]); however, standard installation equipment could not be used because of the small size of the borehole. Instead, 19-mm (0.75-in) polyvinyl chloride (PVC) pipe sections were assembled and marked at the collar end so that the instrument could be properly oriented in the borehole. The PVC pipe was left in place and wedged at the collar. Mindata Pre-Formulated Epoxy Glue Pack HIC—0220 was used to bond the gauge to the wall of the borehole.

The cable wires were connected to a Campbell Scientific CR10X datalogger via a multiplexer. Monitoring of the gauges began immediately (July 30, 1998) after they were installed and the wires connected to the datalogger. Monitoring continued until early morning of Aug. 7, 1998, when the gauge was destroyed by blasting.

Table 1.—Initial and final strain measurements and change in strain resulting from overcoring HICell, microstrain

Measurement description	Gauge number											
	1	2	3	4	5	6	7	8	9	10	11	12
Initial readings	1	7	8	5	7	10	-2	7	3	6	7	7
Final readings	60	228	155	253	283	498	75	130	91	138	330	98
Strain changes	59	221	147	248	276	488	77	123	88	132	323	91

Table 2.—Strain measured at 0 MPa (0 psi) and -10.3 MPa (-1500 psi) during biaxial test on overcore, microstrain

Measurement description	Gauge number											
	1	2	3	4	5	6	7	8	9	10	11	12
0 MPa	1	-4	-6	-4	-6	-5	-7	-2	-7	-3	-2	0
-10.3 MPa	67	-204	-82	-71	-89	-217	55	-208	-87	-85	-201	-204
Strain changes	66	-200	-76	-67	-83	-212	62	-206	-80	-82	-199	-204

Table 3.—Stress components determined by least squares fit to overcoring strains

Stress component	Mine coordinate system		Drift coordinate system	
	MPa	psi	MPa	psi
Normal north-south	-22.76	-3301	-18.34	-2660
Normal east-west	-18.46	-2677	-22.88	-3318
Normal vertical	-12.12	-1758	-12.12	-1758
Shear north-south/east-west	-0.717	-104	-0.062	-9
Shear east-west/vertical	0.438	64	1.572	228
Shear vertical/north-south	-1.673	-243	0.722	105

Table 4.—Principal stresses calculated from fitted stress components

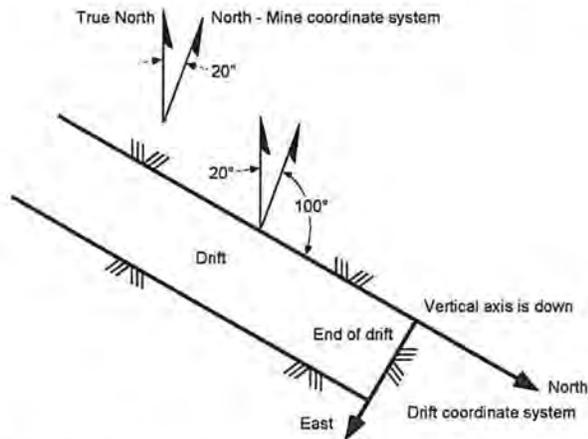| Stress component	Principal stress		Mine coordinate system		Drift coordinate system	
	MPa	psi	Azimuth, deg	Inclination, deg	Azimuth, deg	Inclination, deg
PS1	-11.82	-1714	152.3	79.9	52.3	79.9
PS2	-18.41	-2670	277.1	5.8	177.1	5.8
PS3	-23.11	-3351	8.0	8.3	268.0	8.3

Figure 6.—Drift coordinate system shown in plan view with respect to mine coordinate system and true north
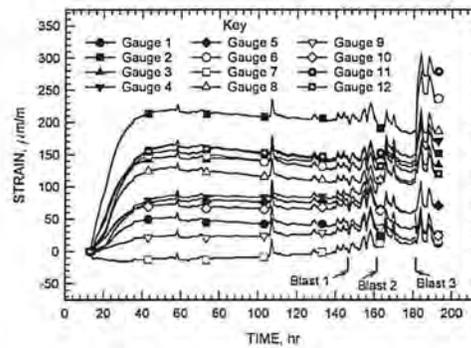

Figure 7.—Time versus measured HICell strains covering period of drift advance

6.2 *Strain Results*

Figure 7 shows measured strains collected during the monitoring period. Measurements made during the first 20 hr of monitoring show response to the exothermic reaction of the glue curing. Measurements taken during the next 95 hr show a relatively smooth curve with clear trends and occasional spikes. After hour 128, all gauges showed similar noise that masked the immediate strain responses resulting from advancing the drift. It was assumed that the noise made the same contribution to every measurement in any one scan. Thus, for any gauge,

$$m_i = \epsilon_i + e \tag{1}$$

where m_i = measurement of gauge i,

ϵ_i = strain contribution,

and e = noise contribution.

Here, e is the same for each gauge, but changes with time.

On the basis of the data shown in Figure 7, most of the response of gauge 7 appeared to be noise. Therefore, if gauge 7 measurements are subtracted from measurements from the other gauges, a preliminary estimate of strain history is obtained (Figure 8). Strain increases imperceptibly during the first advance, but increases abruptly during the second and third face advances. Background noise was approximately the same for every gauge. Figure 8 shows that equation 1 is a reasonable model. The jumps provide preliminary estimates of strains resulting from each blast.

6.3 *Analysis of Strain Results*

The measurements shown in Figure 8 contain errors if gauge 7 strains are nonzero. To eliminate that error, Nichols & Johnson (1998) used two statistical fitting techniques to separate structured noise from strain signals. These methods were singular value decomposition (SVD) and principal component analysis (PCA).
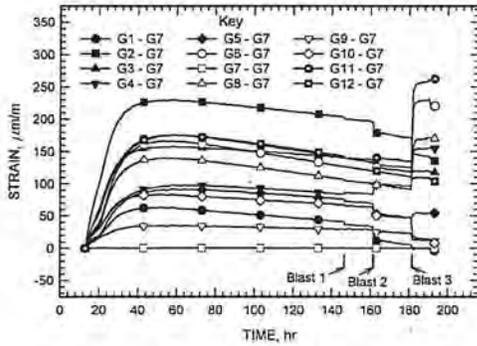
Figure 8.—Time versus measured HICell strains less gauge 7 measurements
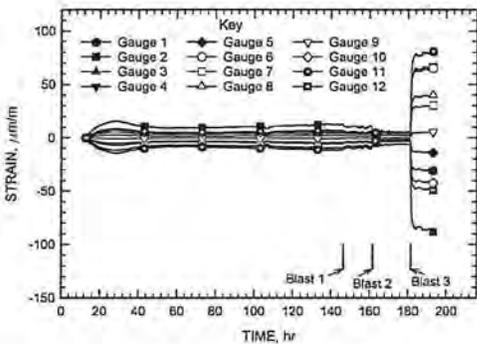

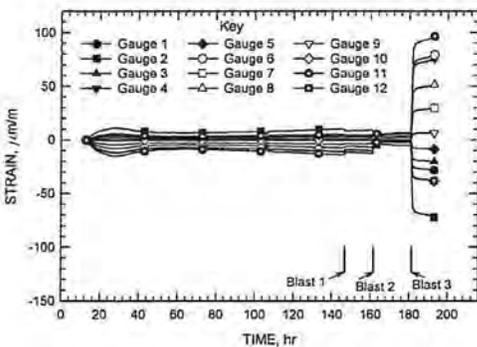Figure 9.—HICell strains over time calculated with SVD to extract external signal

Figure 10.—HICell strains over time calculated with PCA to extract external signal

Figures 9 and 10 show the history of strains computed by SVD and PCA, respectively. The increases in strain immediately after the first blast are nearly imperceptible, especially in the SVD computation, whereas the increase in strain after the second blast is more noticeable. The third increase is considerably larger than the changes shown following the first two blasts. The PCA curves

are smoother than the SVD curves, which indicates that PCA may be a better fit method to use with these data.

Table 5 lists the strain jumps associated with each blast as calculated by SVD and PCA. As stated, there appear to be less noise in the PCA-fitted strains than in the SVD-fitted strains. However, when comparing SVD-fitted strains with PCA-fitted strains, the correlation coefficients were 0.99 for both blasts 2 and 3. This shows that strains computed using both SVD and PCA are not significantly different from each other.

6.4 Stress Change Calculations

Stress changes were fit by using the least squares method along with the computer program STRESsOUT (Larson, 1992) and checked with the program STRESS91 (Mindata, Ltd., 1990). In this report, positive strain change indicates a decrease in compressive strain, and positive stress change indicates a decrease in compressive stress. Elastic material properties used in the calculations were determined from the aforementioned biaxial compression test.

Stress change components were fit to strain changes determined by SVD and PCA for all strain gauges. The correlation coefficients, r^2, for all fits of SVD- and PCA-determined stress changes were 0.90 and 0.91. The standard errors of measurement ranged from 10% to 40% and from 8% to 31% of the highest principal stress change calculated from SVD- and PCA-determined strains, respectively. These ranges are not unusual for stress measurements. The correlation coefficients were high considering that noise had to be filtered from the measurements. This suggests that the measurements were of good quality.

6.5 Analysis of Stress Change

6.5.1. Elastic Continuum Model

A three-dimensional, finite-element continuum model was constructed for the code UTAH3 to assess stresses around a homogeneous, linear-elastic medium. The drift coordinate system was selected for constructing the model because it was easy to use. The mesh was 20.1 m (66 ft) parallel to the drift, 18.3 m (60 ft) parallel to the face, and 18.3 m (60 ft) in the vertical direction. Element size was 0.3 m (1 ft) along any edge. The model contained 237,600 elements, each of which was assigned the in situ stress state as an initial condition. Elastic modulus was 55.2 GPa (8 million psi), which had been measured previously using a Goodman jack. Poisson's ratio was 0.3. Far-field displacements were fixed. Excavation of the initial face perturbed the stress state only slightly (less than or equal to 1.3% of the largest compressive principal stress) at the approximate location of the HICell.

In the constructed mesh, the centroid of the element nearest the HICell was 0.3 m (1 ft) from the north rib line and 1.4 m (4.5 ft) above the plane of the floor. Distance to the face between the model and the field location differed by as much as 0.44 m (1.45 ft). While this difference introduced some error between modeled and measured stresses, the errors were small enough to allow a useful comparison.

In general, the elastic model showed that as the face advanced, the stress normal to the face decreased in compression, while stresses parallel to the face increased in compression.

Table 5.—Strain jumps calculated by SVD and PCA associated with drift advance

Gauge no.	Singular value decomposition analysis			Principal component analysis		
	Blast 1	Blast 2	Blast 3	Blast 1	Blast 2	Blast 3
1	-0.6	-5.7	-24.4	-0.8	-5.1	-22.6
2	-1.8	-16.1	-69.6	-2.1	-13.1	-57.8
3	-0.6	-5.7	-24.6	-0.6	-3.7	-16.1
4	1.4	12.4	53.4	2.2	13.8	60.6
5	-0.3	-2.5	-11.0	-0.2	-1.5	-6.8
6	1.3	12.0	51.8	2.3	14.4	63.5
7	0.6	5.6	24.1	0.9	5.4	23.6
8	0.8	7.4	31.8	1.5	9.4	41.2
9	0.1	1.0	4.1	0.2	1.2	5.3
10	-0.9	-7.8	-33.6	-1.1	-7.0	-30.7
11	1.6	14.9	64.3	2.8	17.6	77.3
12	1.0	-9.0	-39.0	-1.1	-6.9	-30.4

6.5.2 *Measured Stress Change*

The results show that only small amounts of stress change resulted from the first two face advances. A greater amount of stress change occurred after the third face advance when the distance from the face to the instrument was 2.3 m (7.5 ft), or about 70% of the drift width of 3.3 m (10.8 ft) at that location. During the third face advance, the largest principal stress change was tensile (reduction in compressive stress). The orientation of this change was approximately 30° counterclockwise (in plan view) from the direction of face advance and inclined about 21° above horizontal, looking ahead of the face. The intermediate principal stress change was also tensile and near horizontal. Only the principal stress change closest to vertical was compressive. The amount of stress change calculated using SVD strains differed from those calculated using PCA strains. However, signs and principal stress change orientations were consistent and remained nearly the same during all three face advances.

Because the HICell monitored during drift advance was only 2.6 m (8.5 ft) from the overcored HICell and the two instruments were about two drift widths from the initial face (Figure 3), it was assumed that the in situ stress measured was a good approximation of the stress state at both HICell locations. Stress changes resulting from face advance can be added to in situ stress to approximate the progression of stress as the face approached the HICell.

Figures 11 and 12 show the amount of normal and shear stresses in the drift coordinate system as calculated from SVD- and PCA-determined strains versus distance from the face. Also shown in the figures are stresses calculated with the elastic model. Measured horizontal normal stress parallel to the face differs significantly from that calculated with the elastic model. Moreover, as the face approaches the instruments, the significance of the trend becomes opposite that expressed in the elastic model. that is, stress relaxes instead of being concentrated. Other normal stresses are roughly in agreement with the elastic model.

Vertical shear stresses differ from vertical stresses calculated with the elastic model, and as the face approaches the instruments, the trend becomes opposite in sign from that in the elastic model. Horizontal shear stress tracks stress calculated by the model.
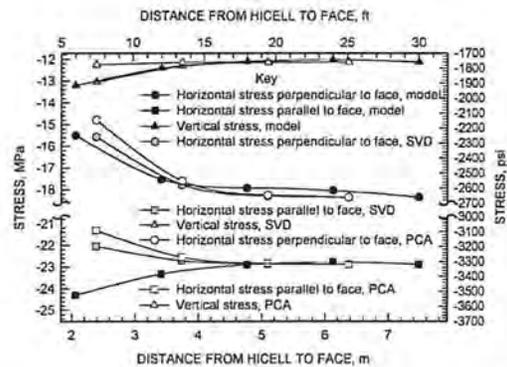

Figure 11 .—Measured normal stresses parallel and perpendicular to the face at HICell location versus distance to face. Measured stresses were calculated with the in situ measurement and stress changes calculated with SVD- and PCA-determined strains
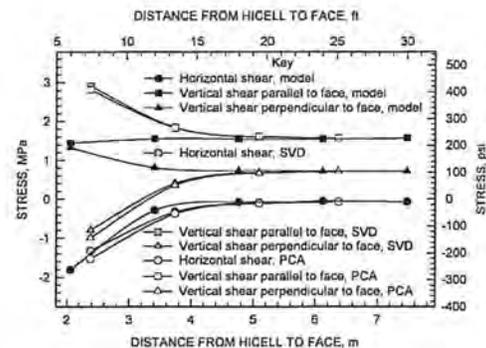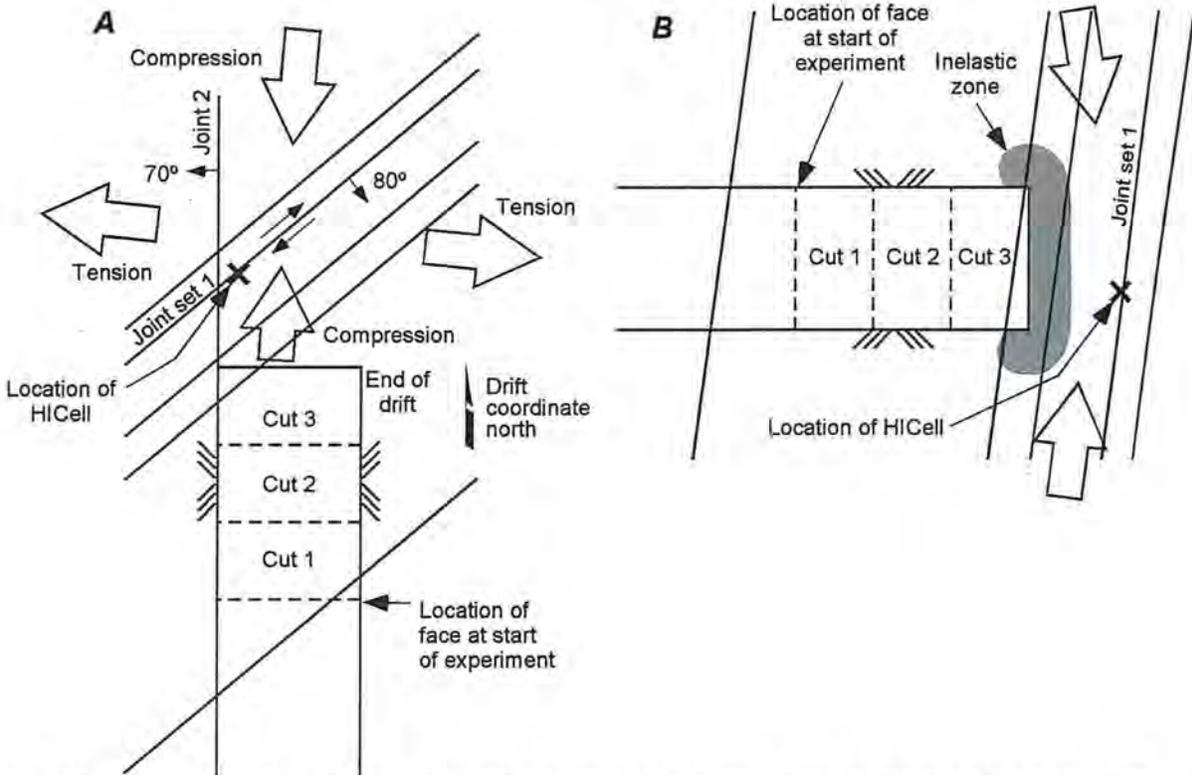

Figure 12.—Measured shear stresses in drift coordinate system at HICell location versus distance to face. Measured stresses were calculated with the in situ measurement and stress changes calculated with SVD- and PCA-determined strains.

Figure 13.—Deformation patterns and resulting deviations of stress from the elastic model. *A*, Plan view of end of drift showing how a shear slip on joint set 1 can cause stress deviations; *B*, Vertical section through drift, HICell, and joints in set 1 showing how an inelastic zone near the face can push stress trajectories further ahead of the face.

There are at least two distinct joint sets near the HICell (Figure 3). The first set strikes N30°W (in the mine coordinate system) and dips 80° to the southwest. The second set strikes S80°E, or roughly parallel to the drift, and dips 70° to the north. A third joint set strikes S88°E and dips 23° to the south. However, joints of this set did not enter the tested rock volume.

The driving mechanisms for the differences between measured and calculated stresses cannot be determined without an extensive study of the influence of these joints and the possible existence of inelastic processes. Even so, it is useful to point out that deviations are consistent with the deformation patterns shown in Figure 13.

The first of these patterns is shear deformation along joint set 1, as indicated by relief of compressive stress parallel to the face and an increase in compressive stress perpendicular to the face (see Figure 13*A*). The increase in compressive stress would not be as much as the increase in tensile stress because of the free face. This deformation is not likely to be slip being driven by static stress. The elastic model indicates a mobilized friction angle of only 14° after the third face advance. Although the friction angle was measured at this mine, 14° is considered too small to have allowed slip. Any slip that did occur had to have been driven by blasting. However, assuming that shear stiffness of the joints was smaller than stiffness of the intact rock, shear softening could have allowed enough shear deformation (not slip) to occur and cause stress deviations.

The second deformation pattern was inferred from differences between the measured vertical shear stresses and those calculated with the elastic model. Gravity was the driving force, while some inelastic vertical deformation near the face (Figure 13*B*) forced vertical stress trajectories away from the face, causing increased vertical shear stresses at the HICell.

7. CONCLUSIONS

In situ stress was successfully measured ahead of the eastern footwall drift in the Stillwater Mine. The near-vertical principal stress was not much different from expected overburden stress. The principal stresses nearest the horizontal plane are closely aligned with regional geologic structures. More measurements are needed to determine a more complete picture of the stress field throughout the mine.

In spite of the presence of an external signal in the data, the SVD and PCA methods of removing noise produced reasonable estimates of changes in strain resulting from face advance. Stress changes derived from these strains calculated using the least squares method provided reasonable estimates of the stress change tensor at the point where the HICell had been installed.

Although the stress response to excavation appeared to be in the elastic range, some components departed from those calculated for an elastic, homogeneous medium. These departures involved the direction, as well as magnitude, of the stress change. Horizontal shear displacement across joint set 1 is consistent with the difference in horizontal normal stress parallel to the face. Inelastic vertical strain near the face, perhaps involving slip on joints that insected the face, is suggested by the increased level of shear stresses. Modeling studies are planned to investigate the deformation and its potential impact on ground control safety.

8. ACKNOWLEDGMENTS

9.   REFERENCES

Larson, Mark. 1992. STRESsOUT—A Data Reduction Program for Inferring Stress State of Rock Having Isotropic Material Properties: A User's Manual, U.S. Bur. Mines Inform. Cir. 9302, 168 pp.

Nichols, T., and S. Johnson. 1998. Noise Reduction of Strain Gauge Data Using SVD, Report SRC-01, 22 pp.

Mindata, Ltd., [1976] CSIRO Hollow Inclusion Stress Cell Field Manual. Mindata, Ltd., Seaford, Australia, 73 pp.

Mindata, Ltd., STRESS91 Users Manual. 1990. Available from Mindata Ltd., Seaford, Australia.

Worotnicki, and R. J. Walton. 1976. Triaxial Hollow Inclusion Gauges for Determination of Rock Stress In Situ, *In* Proceedings, ISRM Symposium on Investigation of Stress in Rock—Advances in Shear Measurement, Sydney, Supplement, pp. 1-8.